Diffuser with pseudorandom phase sequence

Yoshikazu Nakayama and Makoto Kato

Electronics Research Laboratory, Matsushita Electric Industrial Co., Ltd., Moriguchi, Osaka, Japan

(Received 27 February 1979)

A theoretical analysis of the power spectra of diffusers with a series of pseudorandom phase sequences is presented. General equations describing three typical cases of power spectra are derived by making use of the constraints assumed. Profiles of the power spectra showed good agreement with the results of numerical computation using the fast-Fourier-transform algorithm. The images of the diffusers through a double-diffraction optical system were also evaluated by computer simulation. The advantage of pseudorandom phase sequences over random phase sequences is discussed from the viewpoint of signal-to-noise ratio.

INTRODUCTION

The use of diffusers in recording holograms of two-dimensional objects has been studied for improving various aspects of the wave-front reconstruction, such as image quality, redundancy, diffraction efficiency, etc. The role of diffusers is essentially that of coding the object beam with some phase plate which modifies the spatial frequency spectrum of the object information, while giving little effect in the irradiance of the reconstructed image. The phase coding techniques presented so far can be tentatively classified into three types that are based on, respectively, random phase sequences, deterministic phase sequences, and pseudorandom phase sequences (PRPS's). Some typical cases with the former two were analyzed elsewhere in detail.[1-5] A special case of the third type of coding was presented in a previous paper,[6] and consists of four phase levels (0, $\pi/2$, π, $3\pi/2$); phase steps of $\pi/2$ or $-\pi/2$ are repeated at random so that the irradiance fluctuations among the sampling points are more suppressed. The computer simulation of Fourier holography with the random and the pseudorandom diffusers showed improved image quality.[7]

Further development of the pseudorandom diffusers was implemented with special attention to the forms of the power spectra corresponding to the respective phase sequences. As an interesting result of the discussions, a new type of PRPS was derived by modifying the three-level PRPS such that the power spectrum was strictly band-limited by itself.[8]

The purpose of this paper is to approach these problems from an analytical point of view, which makes it possible to design a class of diffusers effective for various optical systems including diffraction-limited holography. We will show explicitly that the forms of the power spectra are controlled preferably by choosing a suitable PRPS. We will also evaluate the signal-to-noise ratio (S/N) of the reconstructed images with given PRPS and given aperture size of the holograms.

I. FRAMEWORK OF ANALYSIS

Figure 1 illustrates a one-dimensional setup of a double diffraction optical system; an object transparency at the plane P_1 is imaged by a pair of Fourier transform lenses L_1 and L_2 onto the plane P_2, in which an aperture of size D_H is placed at the spectrum plane H_m. The optical system described here simulates conveniently a typical case of Fourier holography, if the characteristic of the recording media is neglected. The aperture size D_H corresponds to that of the holograms.

We begin our analysis by assuming that a diffuser with amplitude transmittance $g(x_1)$ is given at the object plane P_1, and is illuminated by plane-parallel light of wavelength λ. The object other than the diffuser is abbreviated in order to derive just the fundamental performances of the diffusers. The results of the analysis, however, allow us to estimate the results for most continuous tone objects since, if such object transparencies are superposed with the diffuser, the modified spectrum distribution of the objects would be governed predominantly by the characteristic of the diffuser.

Now the complex amplitude distribution $G(\xi)$ at the plane H_m is proportional to the Fourier transform of $g(x_1)$. Omitting a constant factor, we have

$$G(\xi) = \int_{-\infty}^{\infty} g(x_1) \exp\left(2\pi i \frac{\xi}{\lambda f} x_1\right) dx_1. \tag{1}$$

The irradiance distribution $I_H(\xi)$ at the plane H_m is

$$I_H(\xi) = G(\xi) \cdot G(\xi)^*, \tag{2}$$

where the asterisk denotes the complex conjugate. The amplitude $t(\xi)$ of the aperture at the plane H_m is, using the rectangle function,[9]

$$t(\xi) = \text{rect}\,(\xi/D_H), \tag{3}$$

so that the irradiance of the band-limited image at the plane P_2 is given by

$$I_2(x_2) = \left| \int_{-\infty}^{\infty} t(\xi) \cdot G(\xi) \exp\left(2\pi i \frac{x_2}{\lambda f} \xi\right) d\xi \right|^2. \tag{4}$$

Let us define a one-dimensional model of the diffuser that consists of $2N + 1$ sampling areas with width L and period P, to which each term of a phase sequence $\{\phi_{-N}, \phi_{-N+1}, \cdots, \phi_0, \cdots, \phi_{N-1}, \phi_N\}$ is associated respectively, as shown in Fig. 2.

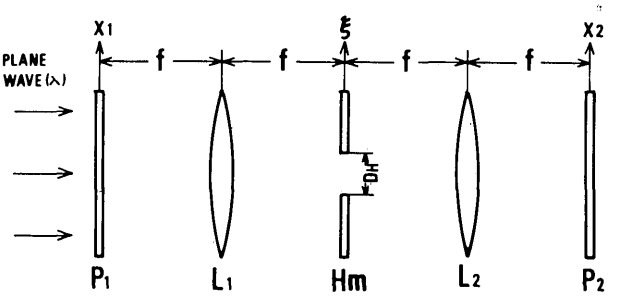

FIG. 1. Double-diffraction optical system. An object at the plane P_1 is imaged through an aperture of the size D_H onto the plane P_2.

 0030-3941/79/101367-06$00.50

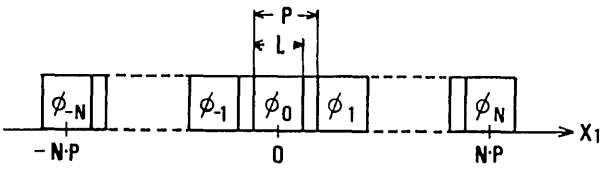

FIG. 2. Schematic model of a one-dimensional diffuser with a pseudo-random phase sequence.

Then, the amplitude transmittance of the diffuser is

$$g(x_1) = \sum_{n=-N}^{N} \mathrm{rect}\left(\frac{x_1 - nP}{L}\right) \exp(i\phi_n), \tag{5}$$

where ϕ_n denotes the phase shift corresponding to the nth sampling area. Here the essential property of the phase sequence under consideration is generally expressed in terms of the constraint

$$\phi_n - \phi_{n-1} = 2\pi/S$$

or

$$2\pi(S-1)/S, \tag{6}$$

where S represents the number of the phase levels. The cases of phase differences $-2\pi/S$ and $-2\pi(S-1)/S$ are considered to be equal to $2\pi(S-1)/S$ and $2\pi/S$, respectively. We express phase differences and phase levels by positive values hereafter. Further, it is assumed that the occurrence of the phase difference $2\pi/S$ or $2\pi(S-1)/S$ arises with equal probability $\frac{1}{2}$ for a sufficiently large number N.

We now define, for the convenience of our analysis, the autocorrelation function of $g(x_1)$;

$$A(x_1) = \int_{-\infty}^{\infty} g(u) \cdot g^*(u - x_1)\, du. \tag{7}$$

According to the autocorrelation theorem, the Fourier transform of $A(x_1)$ is the squared modulus of the Fourier transform of $g(x_1)$, so that we have, from Eqs. (1) and (2),

$$I_H(\xi) = \int_{-\infty}^{\infty} A(x_1) \exp\left(2\pi i \frac{\xi}{\lambda f} x_1\right) dx_1. \tag{8}$$

Substituting Eq. (5) for Eq. (7), we obtain

$$A(x_1) = (2N+1)B(x_1) + \sum_{M=1}^{2N} \sum_{n=-N+M}^{N} \{B(x_1 - MP) \times \exp[i(\phi_n - \phi_{n-M})] + B(x_1 + MP) \times \exp[i(\phi_n - \phi_{n+M})]\}, \tag{9}$$

where

$$B(x_1 \pm MP) = \int_{-\infty}^{\infty} \mathrm{rect}\left(\frac{u}{L}\right) \mathrm{rect}\left(\frac{u - x_1 \mp MP}{L}\right) du, \tag{10}$$

and $\phi_n - \phi_{n\pm M}$ can take any of the values $0, 2\pi/S, 2\pi\cdot 2/S, \ldots,$ and $2\pi(S-1)/S$, with a probability depending on M and the phase difference $\phi_n - \phi_{n\pm M}$.

II. ANALYSIS OF POWER SPECTRA

In this section, we first examine the algebraic formulas that apply to ideal forms of the power spectra for the three-level and the four-level PRPS, namely corresponding to $S = 3$ and $S = 4$, respectively, in Eq. (6). Then we formalize the special case with a six-level complex pseudorandom phase sequence (CPRPS) by modifying the case with $S = 3$. Examples of these three types of phase sequences are listed in Table I.

TABLE I. Examples of the PRPS.

Type of sequence	Phase sequence
4-L-PRPS	$0, \frac{1}{2}\pi, 0, \frac{1}{2}\pi, \pi, \frac{3}{2}\pi, 0, \frac{3}{2}\pi$
3-L-PRPS	$\frac{2}{3}\pi, 0, \frac{4}{3}\pi, \frac{2}{3}\pi, 0, \frac{2}{3}\pi, \frac{4}{3}\pi, \frac{2}{3}\pi$
6-L-CPRPS	$\frac{2}{3}\pi, \frac{1}{3}\pi, 0, \frac{5}{3}\pi, \frac{4}{3}\pi, \pi, \frac{2}{3}\pi, \frac{1}{3}\pi$

A. Four-level PRPS

In the case of the four-level PRPS, Eq. (6) is reduced to

$$\phi_n - \phi_{n-1} = \pi/2$$

or

$$(3/2)\,\pi. \tag{11}$$

We see that the phase difference $\phi_n - \phi_{n-M}$ falls into one of the four levels $(0, \pi/2, \pi, 3\pi/2)$ with a probability depending on M and its phase value as discussed before; for example, $\phi_n - \phi_{n-2}$ and $\phi_n - \phi_{n+2}$ become either 0 or π with equal probability. Calculation of Eqs. (9) and (8) under the constraint of Eq. (11), however, requires the complete set of the probabilities that describe the case other than $\phi_n - \phi_{n\pm1}$ and $\phi_n - \phi_{n\pm2}$. Therefore we define the probability $P_r(J, M)$ that the terms $\phi_n - \phi_{n\pm M}$ have the phase $\pi J/2$ $(J = 0, 1, 2, 3)$, which can be derived as shown in Table II.

The autocorrelation function (9) can be evaluated in the form of the expected value $E[A(X_1)]$ instead of $A(x_1)$ by making use of the probability function $P_r(J,M)$ defined above. We have

$$\begin{aligned} A(x_1) = {} & (2N+1)B(x_1) \\ & + 2N[B(x_1 - P) + B(x_1 + P)] \\ & \times [P_r(0,1) + iP_r(1,1) - P_r(2,1) - iP_r(3,1)] \\ & + \cdots \\ & + (2N - M + 1)[B(x_1 - MP) + B(x_1 + MP)] \\ & \times [P_r(0,M) + iP_r(1,M) - P_r(2,M) - iP_r(3,M)] \\ & + \cdots \\ & + [B(x_1 - 2NP) + B(x_1 + 2NP)] \\ & \times [P_r(0,2N) + iP_r(1,2N) - P_r(2,2N) - iP_r(3,2N)]. \end{aligned} \tag{12}$$

TABLE II. Values of the probability $P_r(J,M)$ that $\phi_n - \phi_{n\pm M}$ in the four-level PRPS takes values $\pi J/2$ $(J = 0,1,2,3)$.

J \ M	1	2	3	-----	M	---
0	0	$\frac{1}{2}$	0		$\frac{1+(-1)^M}{4}$	
1	$\frac{1}{2}$	0	$\frac{1}{2}$		$\frac{1-(-1)^M}{4}$	
2	0	$\frac{1}{2}$	0		$\frac{1+(-1)^M}{4}$	
3	$\frac{1}{2}$	0	$\frac{1}{2}$		$\frac{1-(-1)^M}{4}$	

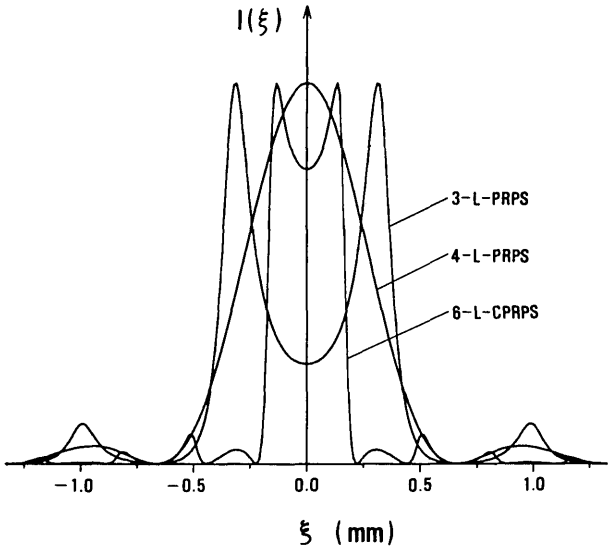

FIG. 3. Normalized forms of the power spectra for the respective diffusers with three typical phase sequences; $L = P = 50\ \mu$, $\lambda = 488$ nm, and $f = 70$ mm.

The first term in Eq. (12) indicates the autocorrelation of one sampling area multiplied by the total number of the sampling areas, and the remaining terms relate to the correlations between a sampling area and the other sampling areas. Using the respective values of $P_r(J,M)$ given by Table II, we obtain

$$E[A(x_1)] = (2N + 1)\, B(x_1). \tag{13}$$

Equation (13) is the same as the result for the random phase sequence of $(0,\pi)$ calcualted by Burckhardt.[1] Substituting Eq. (13) for Eq. (8), we have the irradiance distribution in the plane H_m

$$E[I_H(\xi)] = (2N + 1)L^2 \mathrm{sinc}^2(L\ \xi/\lambda f), \tag{14}$$

where

$$\mathrm{sinc}(L\ \xi/\lambda f) = \frac{\sin(\pi L\ \xi/\lambda f)}{\pi L \xi/\lambda f}.$$

Equation (14) shows that the power spectrum of the four-level PRPS is equal to that of one sampling are multiplied by the number of the sampling areas.

The power spectrum calculated from Eq. (14) is shown in Fig. 3. The corresponding profile (4-L-PRPS) suitably normalized is plotted as a function of ξ, in which parameters $L = 50\ \mu$, $\lambda = 488$ nm and $f = 70$ mm are assumed by way of an example. It is noticed that the width between the first two zeros of this profile is $2\lambda f/L = 1.37$ mm, which corresponds to the Airy disc of one sampling area, if the aperture is circular. The other forms of the power spectrum will be explained in the following sections.

B. Three-level PRPS

The essential condition for the three-level PRPS is

$$\phi_n - \phi_{n-1} = 2\pi/3$$

or

$$(4/3)\pi \tag{15}$$

If we modify the definition of $P_r(J,M)$ as the probability that the phase difference $\phi_n - \phi_{n\pm M}$ becomes $2\pi J/3$ $(J = 0,1,2)$, the probabilities corresponding to J and M are again given as listed in Table III. By making use of $P_r(J,M)$, the autocorrelation function Eq. (9) becomes

$$\begin{aligned}
E[A(x_1)] &= (2N + 1)B(x_1) \\
&\quad + 2N[B(x_1 - P) + B(x_1 + P)] \\
&\quad \times \left[P_r(0,1) + P_r(1,1)\exp\left(i\frac{2}{3}\pi\right) + P_r(2,1)\exp\left(i\frac{4}{3}\pi\right)\right] \\
&\quad + \cdots \\
&\quad + (2N - M + 1)[B(x_1 - MP) + B(x_1 + MP)] \\
&\quad \times \left[P_r(0,M) + P_r(1,M)\exp\left(i\frac{2}{3}\pi\right) + P_r(2,M)\exp\left(i\frac{4}{3}\pi\right)\right] \\
&\quad + \cdots \\
&\quad + [B(x_1 - 2NP) + B(x_1 + 2NP)] \\
&\quad \times \left[P_r(0,2N) + P_r(1,2N)\exp\left(i\frac{2}{3}\pi\right)\right. \\
&\quad \left. + P_r(2,2N)\exp\left(i\frac{4}{3}\pi\right)\right].
\end{aligned} \tag{16}$$

Substituting the respective probabilities shown in Table III for Eq. (16), we have

$$\begin{aligned}
E[A(x_1)] &= (2N + 1)B(x_1) \\
&\quad + \sum_{M=1}^{2N} (2N - M + 1)[B(x_1 - MP) + B(x_1 + MP)] \\
&\quad \times \left(\sum_{k=0}^{[M/2-1]} 2^{-2k-1} - \sum_{k=0}^{[(M-1)/2]} 2^{-2k-1} \right. \\
&\quad \left. + \sum_{k=1}^{[M/2]} 2^{-2k} - \sum_{k=1}^{[(M-1)/2]} 2^{-2k}\right) \\
&= (2N + 1)B(x_1) + \sum_{M=1}^{2N} (2N - M + 1)\left(\frac{-1}{2}\right)^M \\
&\quad \times [B(x_1 - MP) + B(x_1 + MP)],
\end{aligned} \tag{17}$$

where $[g]$ denotes a maximum integer number less than the real number g (Gauss's symbol). Equations (8) and (17) give the power spectrum

$$\begin{aligned}
E[I_H(\xi)] &= \left[2N + 1 + 2\sum_{M=1}^{2N} (2N - M + 1)\left(\frac{-1}{2}\right)^M \right. \\
&\quad \left. \times \cos\left(2\pi MP\frac{\xi}{\lambda f}\right)\right] L^2 \mathrm{sinc}^2\left(L\frac{\xi}{\lambda f}\right).
\end{aligned} \tag{18}$$

The power spectrum calculated from Eq. (18) (3-L-PRPS) is also shown in Fig. 3. The form of this curve suffers a notable

TABLE III. Values of the probability $P_r(J,M)$ that $\phi_n - \phi_{n\pm M}$ in the three-level PRPS takes value $2\pi J/3$ $(J = 0,1,2)$. [ ] denotes Gauss's symbol.

J \ M	1	2	3	-----	M	---
0	0	$\frac{1}{2}$	$\frac{1}{4}$		$\sum_{k=1}^{[M/2]} 2^{-2k+1} - \sum_{k=1}^{[M-1/2]} 2^{-2k}$	
1	$\frac{1}{2}$	$\frac{1}{4}$	$\frac{3}{8}$		$\sum_{k=0}^{[M-1/2]} 2^{-2k-1} - \sum_{k=1}^{[M/2]} 2^{-2k}$	
2	$\frac{1}{2}$	$\frac{1}{4}$	$\frac{3}{8}$		$\sum_{k=0}^{[M-1/2]} 2^{-2k-1} - \sum_{k=1}^{[M/2]} 2^{-2k}$	

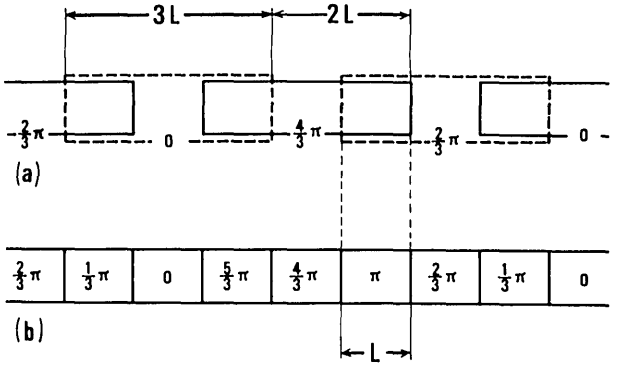

FIG. 4. Relation between the three-level and six-level diffusers; the imaginary three-level diffuser with sampling areas of size $3L$ and period $2L$ (a) is just equivalent to the six-level diffuser with sampling areas of size L and period L (b).

depression in the vicinity of $\xi = 0$, which is due to the fact that the sum of the correlations between a sampling area and other sampling areas in Eq. (17) does not average to zero. Such a depression is directly related to the third term in the square brackets of Eq. (18), which is a periodic function with minima at $\xi = \pm n\lambda f/P$ ($n = 0, 1, 2, \ldots$). The comparison of the two forms corresponding to $S = 3$ and $S = 4$ may suggest a possibility of constructing a more band-limited diffuser, which will be discussed in the next section.

C. Six-level CPRPS

Here we discuss the simple case of the six-level CPRPS, which is obtained by inserting the median phase of the adjacent phase levels between the respective phase terms of the three-level PRPS as illustrated in Table I. We consider that the width L of the sampling areas is equal to the sampling period P of the diffuser. Then the algebraic formula for the power spectrum of the six-level CPRPS can be obtained directly from Eq. (18), if we assume that each width of the sampling area of the three-level PRPS is equal to $3L$, and that the sampling period is $2L$. Such an imaginary extension of the three-level to the six-level phase sequence is explained in Fig. 4, wherein the respective superposed areas of the width L give rise to new phase levels.

Thus we obtain the power spectrum of the six-level diffuser with $2N + 1$ sampling areas from Eq. (18), by replacing $2N$, L, and P with N, $3L$, and $2L$, respectively,

$$E[I_H(\xi)] = 9\left[N + 1 + 2\sum_{M=1}^{N}(N - M + 1)\left(\frac{-1}{2}\right)^M \times \cos\left(4\pi ML\frac{\xi}{\lambda f}\right)\right] L^2\mathrm{sinc}^2\left(3L\frac{\xi}{\lambda f}\right). \quad (19)$$

In the above diffuser, the width of the sampling areas at both the terminals is $2L$. The result, however, is hardly influenced by such irregularities for a sufficiently large number N. Evaluation of Eq. (19) shows that $E[I_H(\xi)]$ drops initially to zero at $\xi = \pm\lambda f/3L$. Thus the width of the main lobe of the power spectrum is reduced to one-third of that given by Eqs. (14) and (18).

The power spectrum which has already been shown in Fig. 3 was actually calculated from Eq. (19), wherein the width $L = P = 50\ \mu$ was assumed.

The absolute ratios of the maxima of the power spectra thus obtained for the four-level, the three-level, and the six-level phase sequences were also found to be 1:1.27:1.95.

III. EVALUATION OF THE DIFFUSERS BY COMPUTER SIMULATION

In this section we evaluate the properties of the respective diffusers by simulating again the optical system shown in Fig. 1, in which computer techniques based on the fast-Fourier transform algorithm are applied. This includes numerical

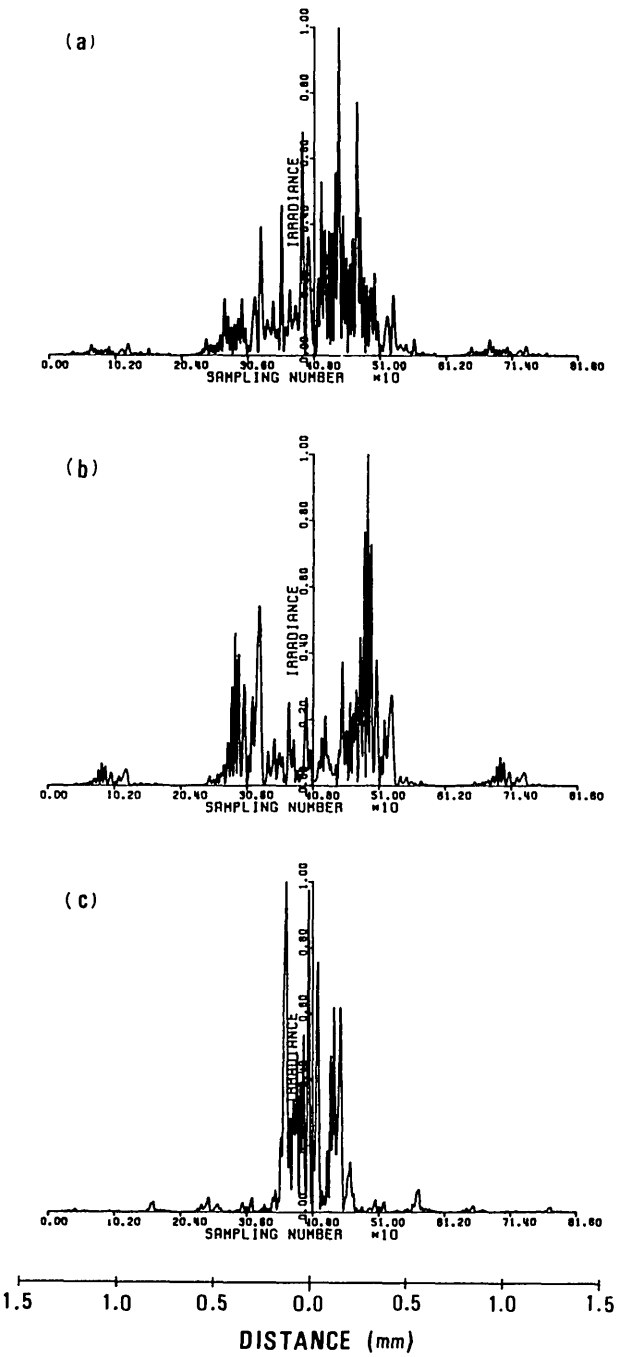

FIG. 5. Power-spectra obtained by a computer simulation: (a), the four-level diffuser; (b), the three-level diffuser; (c), and the six-level diffuser. Other parameters are the same as in Fig. 3.

computations of the irradiance distributions at both the spectrum plane H_m and the image plane P_2. The image quality is evaluated in terms of S/N as defined later. The parameters in these simulations are the same as given in Fig. 3.

The irradiance distributions at the spectrum plane are illustrated in Fig. 5, in which Figs. 5 (a), 5 (b), and 5 (c) show the normalized power spectra of the four-level, the three-level, and the six-level diffuser, respectively. The results are in good agreement with the forms derived by the analytical process. Figure 6 shows the normalized irradiance distributions at the image plane of the four-level diffuser with reference to the original phase levels. The aperture size $D_H = 1.37$ mm is again identical to the width through which the central portion of the Fourier spectrum has just passed. Figure 7 shows similar results for the six-level diffuser, in which the aperture size $D_H = 0.46$ mm corresponds to using the main portion of the power spectrum. It is noted that: (i) the amplitude of the sinusoidal fluctuation in the latter case is considerably smaller than the former; (ii) an almost uniform distribution is obtained in the image plane of the six-level diffuser when the diffraction limited (for the dimension of one period $L = 50\ \mu$) aperture of $D_H = 0.96$ mm is used; and, (iii) random fluctuations in the image of the latter seem to be smaller than in the former case. We will calculate the S/N in order to study quantitatively such behavior of the images. We specify the signal-to-noise ratio

$$S/N = 20 \log_{10} \frac{[I_2'(x_2)]_{\mathrm{av}}}{[(\{I_2'(x_2) - [I_2'(x_2)]_{\mathrm{av}}\}^2)_{\mathrm{av}}]^{1/2}}, \qquad (20)$$

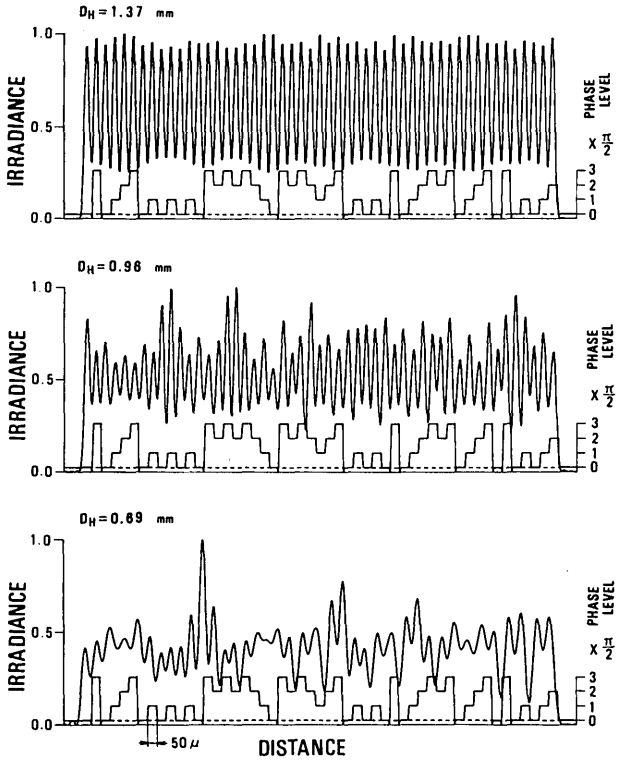

FIG. 6. Original phase levels of the four-level diffuser and their normalized images obtained by a computer simulation. D_H indicates the aperture size corresponding to that of the hologram. Other parameters are the same as in Fig. 3.

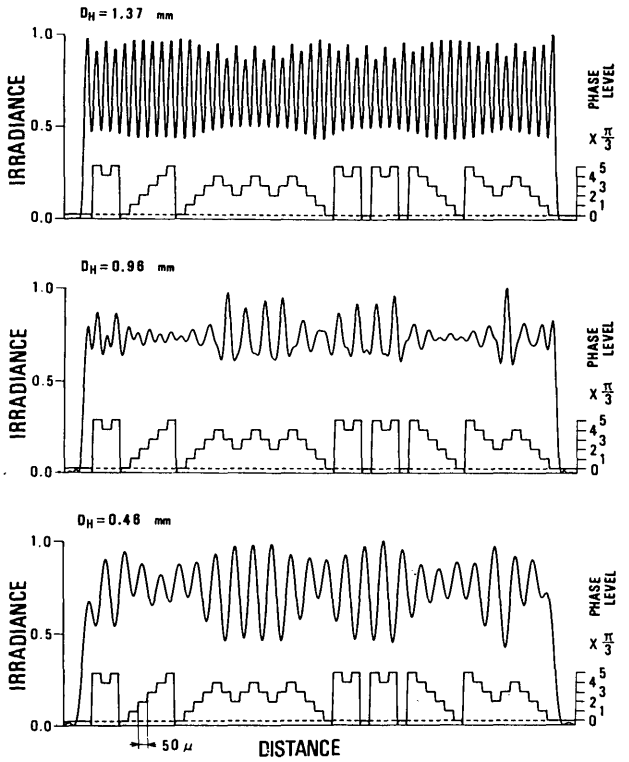

FIG. 7. Original phase levels of the six-level diffuser and their normalized images obtained by a computer simulation. D_H indicates the aperture size corresponding to that of the hologram. Other parameters are also the same as in Fig. 3.

where

$$I_2'(x_2) = \int_{x_2 - P_0/2}^{x_2 + P_0/2} I_2(x_2)\, dx_2, \qquad (21)$$

$[I_2'(x_2)]_{\mathrm{av}}$ denotes the mean value of the irradiance fluctuation, which can be measured if the image is scanned by a photomultiplier with a slit width P_0, and $[(\{I_2'(x_2) - [I_2'(x_2)]_{\mathrm{av}}\}^2)_{\mathrm{av}}]^{1/2}$ is the standard deviation of that irradiance fluctuation. Figure 8 shows the S/N of the images versus the hologram size (D_H) for some typical diffusers, where the S/N was calculated from Eqs. (20) and (21) by assuming $P_0 = 50$

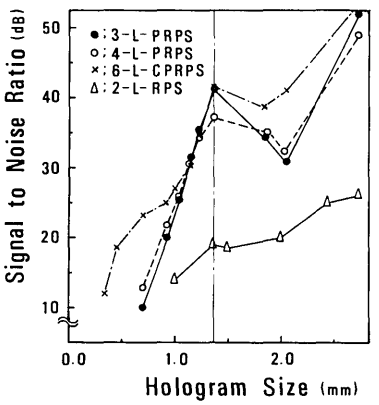

FIG. 8. Calculated signal-to-noise ratio of the image versus hologram size (S/N vs D_H) with respect to the four typical phase sequences; $P_0 = 50\ \mu$ and other parameters are also the same as in Fig. 3.

μ. An optimum size of the hologram is apparently $D_H = 1.37$ mm (chained line) which is equal to the width of the main lobe of the power spectrum for the three-level and the four-level diffuser. It is noticed that the curve for the six-level diffuser keeps better S/N than the other curves at the range of $D_H <$ 1 mm. The approximate period of the regular fluctuation appearing in Fig. 7 ($D_H = 0.96$ mm, $D_H = 0.69$ mm) was about 100 μ, which was twice the period of $P = P_0 = 50\ \mu$; then the S/N of about 42 dB was obtained in the case of $D_H = 0.96$ mm under the modified condition of $P_0 = 100\ \mu$. The S/N for the two-level random-phase sequence $(0,\pi)$ was plotted (2-L-PRS) as a reference for the cases with PRPS.

IV. SUMMARY

In the foregoing analysis of pseudorandom diffusers we have derived the typical forms of the power spectrum for the PRPS including the six-level CPRPS which can yield a spectrum of almost rectangular shape. The results of the analysis were compared with those of numerical computation, and the profiles obtained (Fig. 4 and Fig. 5) showed good agreement with each other.

The double diffraction process was also simulated by numerical computation with respect to the aperture sizes; the signal-to-noise ratio of the images of the respective diffusers was discussed from the viewpoint of the standard deviation of the irradiance fluctuation. In the region of diffraction limited imagery, the six-level diffuser yields a relatively uniform irradiance distribution, which is generally advantageous because: (i) distortion of the images due to moiré between object and the diffuser can be greatly suppressed; and, (ii) the loss of object information is also reduced when the optical image is picked up by some scanning system such as an image tube. It seems hopeful that diffraction-limited holography of continuous tone objects with the S/N, e.g., near 40 dB can be achieved. The effect of the object to be superposed on the diffuser, however, has not been considered here. If the object transparency contains a spatial-frequency bandwidth close to or larger than that of the diffuser, a more detailed analysis and discussion are needed with respect to the specific cases.

The comparison between diffusers with the pseudorandom phase sequences must also take into account the linearity and the dynamic range of the recording media, if, for example, holographic applications are concerned. Those aspects of the diffuser, as well as some experimental results, will be presented in papers to follow.

ACKNOWLEDGMENTS

We wish to thank Mr. I. Sato who offered the S/N curve for two-level random-phase sequence as a reference for the cases with pseudorandom phase sequences. Also, we express our appreciation to Professor T. Suzuki for continuous encouragement.

APPENDIX

Power Spectrum for S-level PRPS

In this appendix we extend the analysis to the general formula of the power spectrum corresponding to the S-level PRPS (S is a number of the quantized phase levels).

As in Sec. I we start with the definition of the probability $P_r(J,M)$ that $\phi_n - \phi_{n\pm M}$ takes value $2\pi J/S$ ($J = 0, 1, 2, \ldots, S-1$). By referring to Tables II and III, $P_r(J,M)$ can be written as

$$P_r(J,M) = (1/2)[P_r(J-1,M-1) + P_r(J+1,M-1)] \tag{22}$$

with the initial condition

$$P_r(J,1) = \begin{cases} 1/2, & J = 1 \text{ or } S-1 \\ 0, & \text{otherwise,} \end{cases} \tag{23}$$

where $P_r(-1,M)$ and $P_r(S,M)$ are considered to be equal to $P_r(S-1,M)$ and $P_r(0,M)$, respectively. The initial condition Eq. (23) is given from Eq. (6). The autocorrelation function Eq. (9) becomes, by making use of $P_r(J,M)$,

$$E[A(x_1)] = (2N+1)B(x_1) + \sum_{M=1}^{2N}(2N-M+1)\sum_{J=0}^{S-1}P_r(J,M)\cos\left(\frac{2\pi}{S}J\right) \times [B(x_1 - MP) + B(x_1 + MP)]. \tag{24}$$

We obtain the final equation by substituting Eq. (24) for Eq. (8),

$$E[I_H(\xi)] = \left[2N+1+2\sum_{M=1}^{2N}(2N-M+1)\sum_{J=0}^{S-1}P_r(J,M) \times \cos\left(\frac{2\pi}{S}J\right)\times\cos\left(2\pi MP\frac{\xi}{\lambda f}\right)\right]L^2\,\mathrm{sinc}^2\left(L\frac{\xi}{\lambda f}\right). \tag{25}$$

Equation (25) is reduced to Eq. (18) or Eq. (14) if we replace S by 3 or 4. It should be noted that the power spectrum is shaped into a sharp form when the integer number S is increased in Eq. (25).

[1]C. B. Burkhardt, "Use of a Random Phase Mask for the Recording of Fourier Transform Holograms of Data Masks," Appl. Opt. **9**, 695–700 (1970).
[2]Y. Takeda, "Random Phase Sifters for Fourier Transformed Holograms," Appl. Opt. **11**, 818–822 (1972).
[3]W. J. Dallas, "Deterministic Diffusers for Holography," Appl. Opt. **12**, 1179–1187 (1973).
[4]S. Yonezawa, "A Deterministic Phase Shifter for Holographic Memory Devices," Opt. Commun. **19**, 370–373 (1976).
[5]Y. Torii, "Synthesis of Deterministic Phase Codes for Phase Shifter in Holography," Opt. Commun. **24**, 157–180 (1978).
[6]M. Kato, Y. Nakayama, and T. Suzuki, "Speckle Reduction in Holography with a Spatially Incoherent Source," Appl. Opt. **14**, 1093–1099 (1975).
[7]I. Sato, and M. Kato, "Speckle-Noise Simulation of Fourier-Transform Holography with Random Phase Sequence," J. Opt. Soc. Am. **65**, 856–857 (1975).
[8]M. Kato, I. Sato, and Y. Nakayama, "Speckle Reduction Processing in Holography," Proceedings of the Tenth Congress of the International Commission for Optics, Palacký University, Olomouc Czech Technical University, Prague, August 25–29, 1975.
[9]J. W. Goodman, *Introduction to Fourier Optics*, (McGraw-Hill, New York, 1968), p. 13.